

# Dielectric Design Optimization of Transformer Windings under Fast Front Excitation

Juan M. Villanueva-Ramírez, Pablo Gómez, Fermín P. Espino-Cortés

**Abstract--**In this paper a procedure is proposed to find an optimized dielectric design of a power transformer winding subjected to a fast front voltage excitation. The procedure is based on the interaction between the Finite Element Method (FEM), a winding model for fast front transient analysis, and a multiobjective optimization algorithm. To validate the results, the dielectric responses before and after optimization are compared for three transformer winding configurations.

**Keywords:** Design optimization, transient voltage response, dielectric stress, transformer winding.

## I. INTRODUCTION

Power transformers are essential elements of electrical power systems. Their design must comply with strict reliability requirements to minimize the probability of failure and satisfy the quality standards of uninterrupted energy supply.

The lightning impulse test defines in typical cases the maximum dielectric stress that the insulation system will withstand and thus, it is used as a reference for the design of transformers [1]. However, the continuous increase in the utilization of power-electronic technologies at different parts of the electrical network has incremented the exposure of transformer windings to fast and repetitive voltage pulses, which can accelerate the deterioration and premature failure of the insulation system of these power components [2], [3], [4].

In this work, a procedure is proposed to find an optimized geometrical configuration of a power transformer winding subjected to a fast front voltage excitation. The optimized design minimizes the probability of premature insulation deterioration or failure while reducing the overall dimensions and cost. The procedure establishes an interaction between the Finite Element Method (FEM), a frequency domain winding model, and the goal attainment optimization algorithm to calculate the parameters, dielectric stress distribution and transient voltage response of the transformer winding. The latter is utilized as the initial voltage condition of the problem to minimize the dielectric stress in the transformer winding.

## II. FREQUENCY DOMAIN TRANSFORMER WINDING MODELING

The transformer winding is modeled using the per-unit-length equivalent circuit illustrated in Fig. 1 [5]. In this figure,  $L$  is the winding series inductance,  $R$  is the series resistance,  $C_s$  is the series capacitance,  $R_s$  is the series dielectric loss component,  $C_g$  is the ground capacitance and  $R_g$  is the ground dielectric loss component.

To accurately calculate the propagation of voltages along the winding, the equivalent circuit is described by a distributed-parameter representation based on the multiconductor transmission line theory in which each conductor represents a turn of the winding [1], [6]. To preserve continuity, the end of each turn is connected to the beginning of the next one by means of a large admittance  $Y_{con}$  ( $1 \times 10^6$  S), resulting in a zig-zag connection, as shown in Fig. 2 [7]. The equivalent impedance  $Z_{eq}$  connected at the receiving end of the  $n$ -th conductor represents the remaining of the winding or the neutral impedance. The reader is referred to [6] for a complete mathematical description and experimental validation of this model.

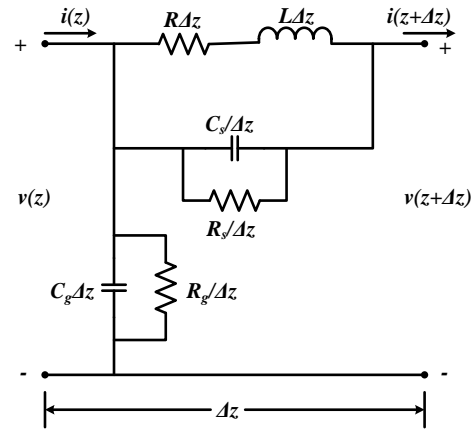


Fig. 1 Per-unit-length equivalent circuit of a transformer winding [5].

## III. CALCULATION OF PARAMETERS

Accurate computation of inductive, capacitive and loss components is required for an adequate prediction of the transformer winding behavior when subjected to very fast transients [7].

### A. Capacitance

The capacitance matrix p.u.l. (per-unit length)  $\mathbf{C}$  of the winding is obtained from electrostatic field simulations on a 2D arrangement using FEM-based software COMSOL Multiphysics applying ground boundaries at the core walls and considering only the section of the coil inside of the core

J. M. Villanueva-Ramírez are with the Department of Electrical and Computer Engineering, Western Michigan University, Kalamazoo, MI 49008 USA (e-mail: [juannm.villanueva@wmich.edu](mailto:juannm.villanueva@wmich.edu), [pablo.gomez@wmich.edu](mailto:pablo.gomez@wmich.edu)).

F. P. Espino-Cortés is with the Department of Electrical Engineering SEPI-ESIME ZAC, Instituto Politécnico Nacional, Mexico City, Mexico (e-mail: [espinooc@ipn.mx](mailto:espinooc@ipn.mx)).

window. Self and mutual capacitances are obtained using the electrostatic energy method, as described in [8].

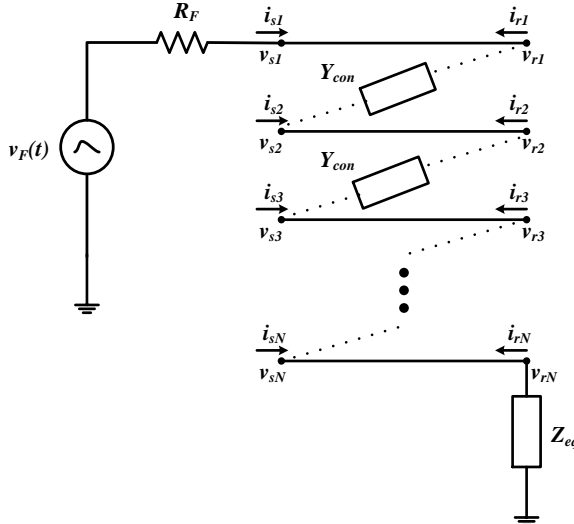


Fig. 2 Multiconductor transmission line model for winding representation [7].

### B. Inductance

The geometrical inductance matrix p.u.l. of the winding is obtained using the inverse of the capacitance matrix considering a homogeneous medium as

$$\mathbf{L} = \mu \epsilon \mathbf{C}^{-1} \quad (1)$$

where  $\mu$  and  $\epsilon$  are the permeability and permittivity of the surrounding medium, respectively.

### C. Losses

Conductor losses p.u.l. due to skin effect considering a rectangular cross section are calculated from the *dc* resistance  $R_{dc}$  and high frequency impedance  $Z_{hf}$  p.u.l., as follows:

$$Z_c = \sqrt{R_{dc}^2 + Z_{hf}^2} \quad (2)$$

where

$$R_{dc} = \frac{\rho_c}{wh}, \quad Z_{hf} = \frac{\rho_c}{2p(w+h)} \quad (3a,b)$$

$\rho_c$  is the resistivity of the conductor material,  $w$  and  $h$  are the conductor width and height, respectively and  $p$  is the complex penetration depth, defined as

$$p = \sqrt{\frac{\rho_c}{j\omega\mu_c}} \quad (4)$$

$\mu_c$  is the conductor's permeability. Furthermore, it is considered that at high frequencies the core acts as magnetic flux barrier; therefore, the flux penetration into the core and associated losses are neglected [9].

## IV. OPTIMIZATION PROCEDURE

The optimization process is divided into several steps

described below. The overall procedure is illustrated by means of the block diagram shown in Fig. 3.

### A. Geometrical Configuration and Parameter Computation

First, the geometry to be optimized is defined in COMSOL Multiphysics based on the distances between adjacent turns, between winding and core, and between layers. The correct selection of material properties, physics and meshing of the problem is of great importance for an adequate performance of the algorithm. Once the geometry has been generated, the electrical parameters of the winding are obtained and introduced into the winding model implemented in MATLAB to compute the transient voltages along the winding.

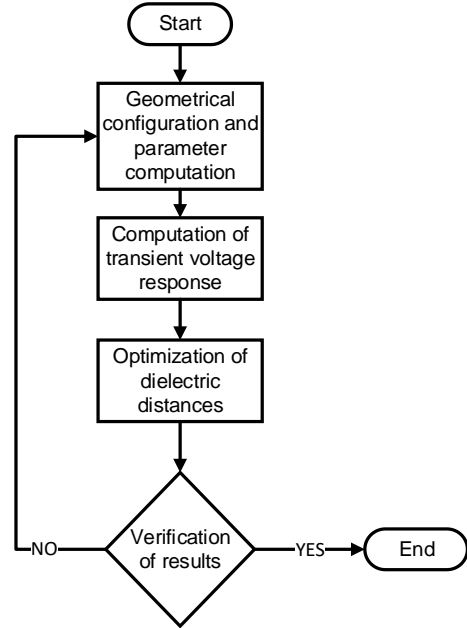


Fig. 3 Block diagram of the optimization procedure

### B. Computation of Transient Voltage Response

Parameters associated with the geometry generated in COMSOL Multiphysics are extracted and used in the frequency domain transformer winding model. The time domain solution of the system is then obtained by means of the numerical inversion of the Laplace transform, as described in [10]. Comparisons between responses of consecutive turns and layers, and between turns and core are performed to obtain the voltages that produce the maximum instantaneous dielectric stress between elements inside the transformer. These values of voltage serve as the initial inputs for the optimization algorithm.

### C. Application of the Optimization Algorithm

A live interface between COMSOL Multiphysics and MATLAB is used to optimize the dimensions of the different regions in the insulation system of the winding. The goal is to minimize the dielectric distances while ensuring that the dielectric stresses produced by the fast front excitation on the obtained geometry will not be higher than one maximum allowed. The goal attainment algorithm (`fgoalattain`) included in the optimization toolbox of MATLAB was

selected to solve the problem due to its capability of obtaining specific values for multiobjective functions. Although this algorithm might provide local solutions, its successive application converged to an adequate result for the test cases discussed in this paper.

#### D. Verification of Results and Iteration

Once an initial solution is achieved, the results are used to compute the transient voltage response corresponding to the optimized geometrical configuration, verifying that the maximum dielectric stress that the insulation system is able to withstand has not been violated and decide if a new iteration is required.

#### V. TEST CASES

Three simplified geometries of transformer winding are used to validate the optimization procedure. The first case (Case A) corresponds to a 1-layer transformer winding consisting of 31 turns with a cross-sectional area of 4 mm x 4 mm and separated by 2mm. The initial geometrical configuration is illustrated in Fig. 4. Core window's height is modified based on the distance between adjacent turns. The second and third cases (Cases B and C) preserve the same geometrical configuration but adding a second and a third layer of conductors with a separation between layers of 2 mm, as shown in Fig. 5.

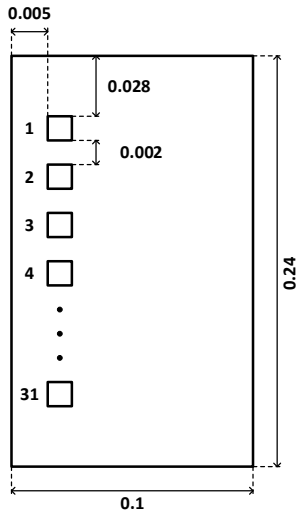


Fig. 4 Geometrical configuration of transformer winding (Case A)

The objective functions for both cases are defined as the maximum dielectric stresses between adjacent turns (Region I), and between winding and core (Region II). For the second and third cases an additional objective function corresponds to the maximum dielectric stress between layers (Region III).

The design parameters are the distances between elements in the 3 regions aforementioned. In contrast to the common application of optimization algorithms for the minimization of a set of objective functions, the procedure applied here intends to find the distances for which specific values of dielectric stress are satisfied. A simplified test value of 34 MV/m is set as the objective in all regions for the optimization algorithm, which corresponds to 85% of the dielectric strength of a

simulated insulation system (40 MV/m). However, for more complex transformer configurations with different insulation materials, different values of dielectric strength can be defined for each region.

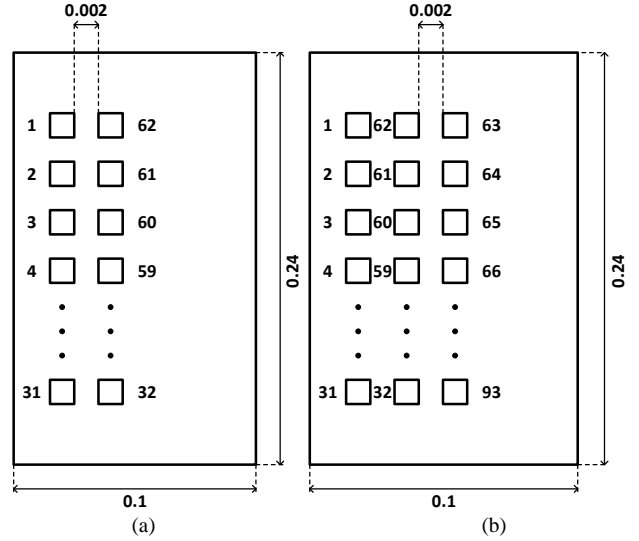


Fig. 5 Geometrical configuration of the transformer winding: (a) Case B, (b) Case C.

The transformer winding model is excited using a double ramp signal with an amplitude of 60 kV, front time of 20 ns and a time to half value of 100  $\mu$ s. The fast rise time of this excitation is intended to emulate the switching characteristics of a modern power-electronic-based converter.

#### VI. RESULTS

##### A. One-Layer Winding

The transient voltage response for the initial geometrical configuration of the one-layer winding is depicted in Fig. 6. From this response, the instant of maximum potential difference between adjacent turns and between winding and core are calculated as follows:

$$\mathbf{V}_{turns} = \max \begin{pmatrix} v_1(t) - v_2(t) \\ v_2(t) - v_3(t) \\ \vdots \\ v_{n-1}(t) - v_n(t) \end{pmatrix} \quad (5a)$$

$$\mathbf{V}_{core} = \max \begin{pmatrix} v_1(t) - V_c \\ v_2(t) - V_c \\ \vdots \\ v_r(t) - V_c \end{pmatrix} \quad (5b)$$

where  $n$  is the number of turns,  $r$  is the number of turns per layer and  $V_c$  is the voltage at the core (or at the low voltage winding for an actual transformer), which is assumed to be zero in the simulation to consider the worst-case scenario. The corresponding voltages are used as the excitation for the geometrical configuration generated in COMSOL Multiphysics to obtain the maximum dielectric stress in

Regions I and II as the initial inputs for the multiobjective optimization problem. Results of the transient voltage response for each turn, dielectric stress and a close-up to the region where the maximum value is located are shown in Figs. 6 to 8 for the initial geometry.

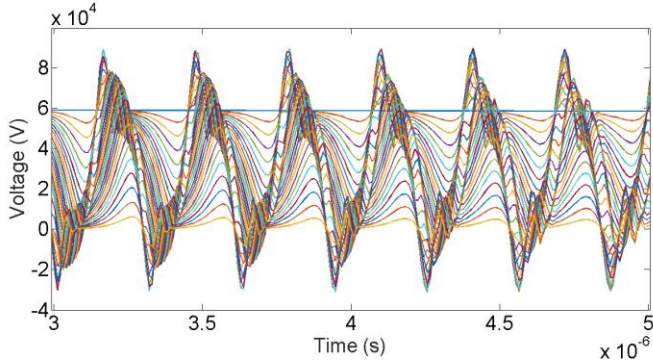


Fig. 6 Transient voltage response at each turn of the transformer winding for the initial geometrical configuration (Case A)

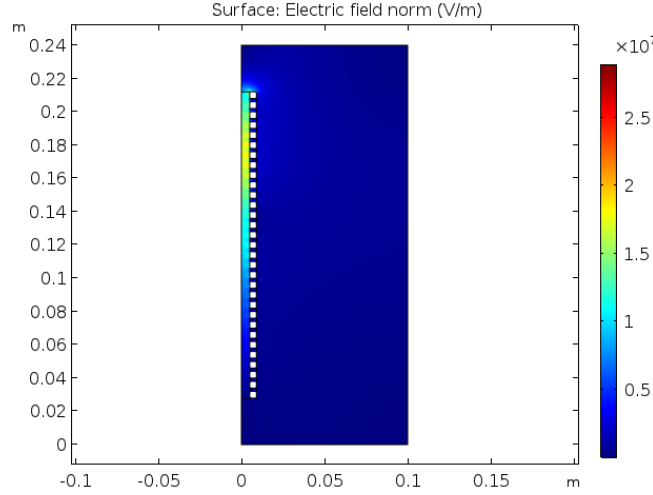


Fig. 7 Dielectric stress distribution of the transformer winding for the initial geometrical configuration (Case A)

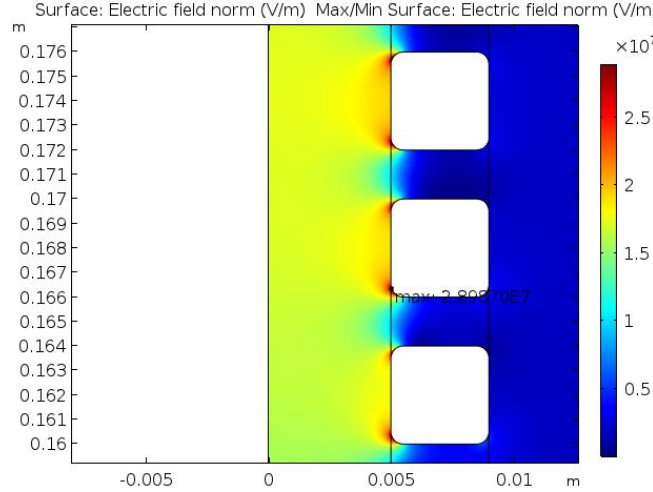


Fig. 8 Close-up to the region of maximum dielectric stress for the initial geometrical configuration (Case A)

As an illustrative comparison, the same plots are presented in Figs. 9 to 11 for the optimized geometry. The dielectric stress and distances between elements in the two regions defined for this case are presented in Table I for the initial and optimized geometrical configurations.

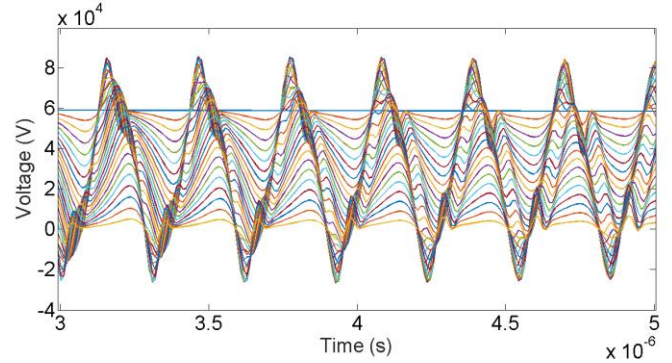


Fig. 9 Transient voltage response at each turn of the transformer winding for the final geometrical configuration (Case A)

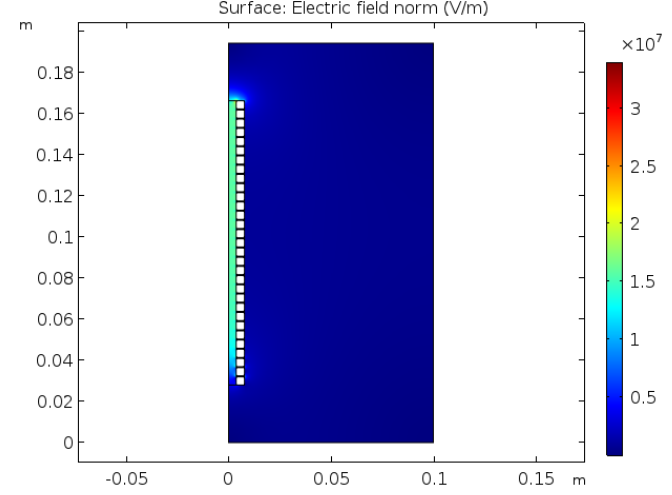


Fig. 10 Dielectric stress distribution of the transformer winding for the final geometrical configuration (Case A)

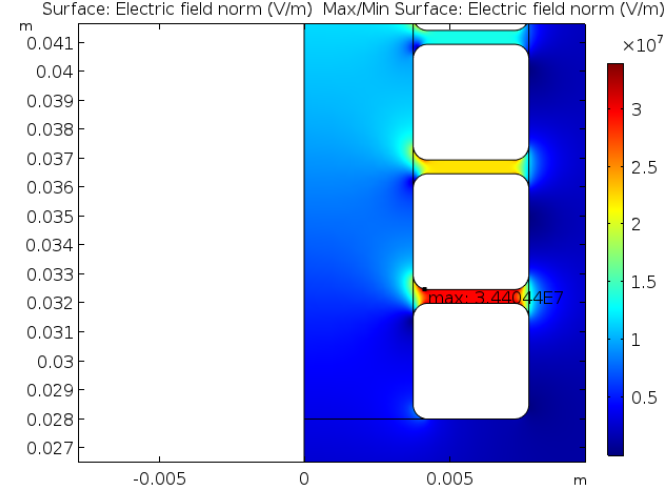


Fig. 11 Close-up to the region of maximum dielectric stress for the final geometrical configuration (Case A)

TABLE I. RESULTS (CASE A)

Geometry	Distance [mm]		Maximum dielectric stress [MV/m]	
	Region I	Region II	Region I	Region II
Initial	2	5	28.987	28.514
Optimized	0.4773	3.761	34.404	34.008

### B. Two-Layer Winding

The transient voltage response for the initial geometrical configuration of the two-layer winding is calculated from the frequency-domain winding model and the inverse NLT. The instant of maximum potential differences between adjacent turns and between winding and core are calculated from this response using equations (5a) and (5b), respectively; and between adjacent layers as:

$$\mathbf{V}_{\text{layers}} = \max \left( \begin{bmatrix} v_1(t) - v_{2r}(t) \\ v_2(t) - v_{2r-1}(t) \\ \vdots \\ v_r(t) - v_{r+1}(t) \end{bmatrix} \right) \quad (5c)$$

The corresponding voltages are used as the excitation of the winding geometry (initial inputs for the optimization algorithm). For sake of simplicity, only results from the optimized configuration are presented in Figs. 12 to 14; however, the dielectric stress and distances between elements in the three regions are presented in Table II for the initial and optimized geometries.

### C. Three-Layer Winding

Results after the optimization procedure for the three-layer configuration are presented in Figs. 15 to 17. In a similar manner to Case B, the dielectric stress and distances between elements are presented in Table III for the initial and optimized geometries.

## VII. DISCUSSION

From the results, it can be seen that the distance between adjacent turns is reduced significantly in all cases, which would be reflected in a substantial reduction in the overall dimensions of the transformer and thus, the weight and cost of manufacturing. Most importantly, the maximum dielectric stress allowed for the insulation material (40 MV/m) is met using the transient voltage response for all three configurations used, which diminishes the possibility of failure once in normal operation and under fast front excitation.

Additional tests were performed using similar excitations with slower front times to verify the validity of the optimized design. In all the cases the maximum dielectric stress remained under the established value defined for each region.

Even though these results are promising, they only constitute the first step in defining an optimization procedure for a practical transformer design in which dielectric, mechanical, thermal and magnetic aspects, and their interaction, must be considered.

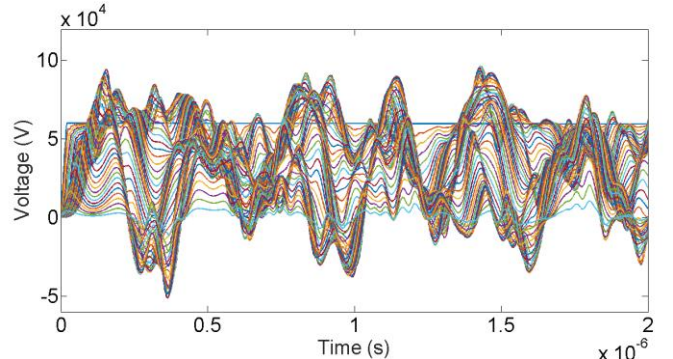


Fig. 12 Transient voltage response at each turn of the transformer winding for the final geometrical configuration (Case B)

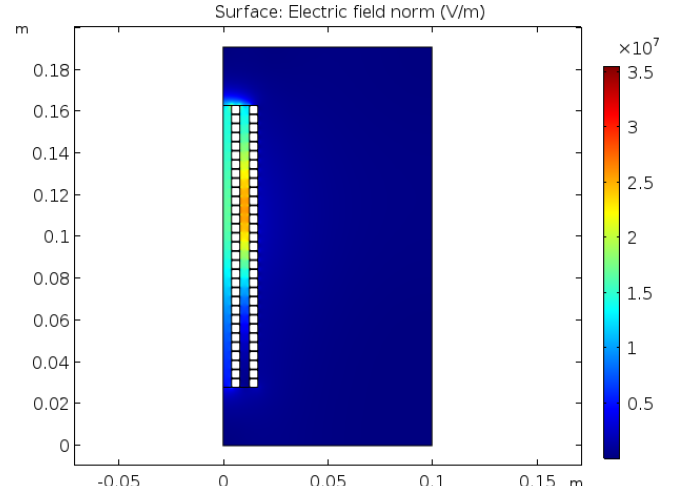


Fig. 13 Dielectric stress distribution of the transformer winding for the final geometrical configuration (Case B)

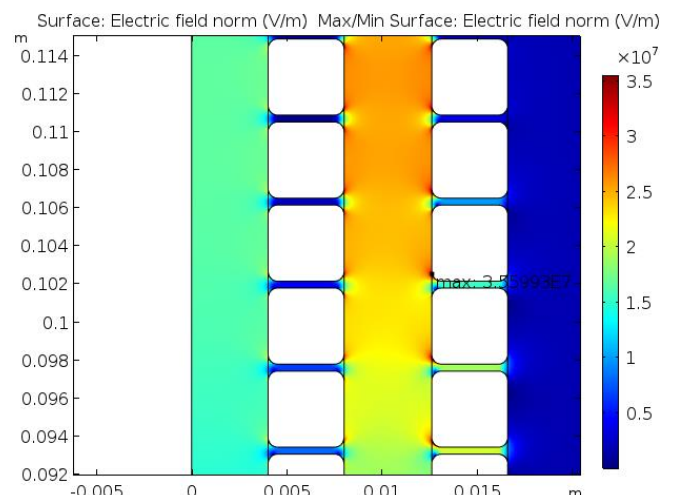


Fig. 14 Close-up to the region of maximum dielectric stress for the final geometrical configuration (Case B)

TABLE II. RESULTS (CASE B)

Geometry	Distance [mm]			Maximum dielectric stress [MV/m]		
	Region I	Region II	Region III	Region I	Region II	Region III
Initial	2	5	2	77.698	31.34	75.983
Optimized	0.362	4.027	4.616	35.599	34.266	34.95

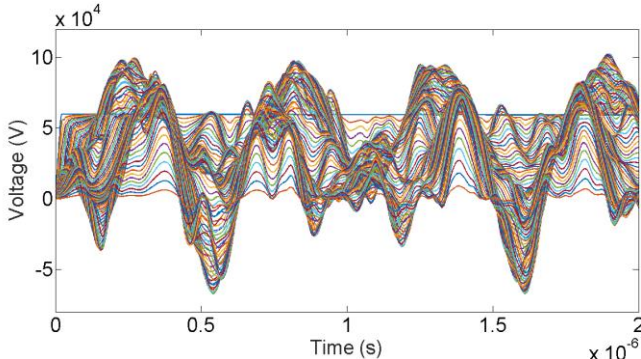


Fig. 15 Transient voltage response at each turn of the transformer winding for the final geometrical configuration (Case C)

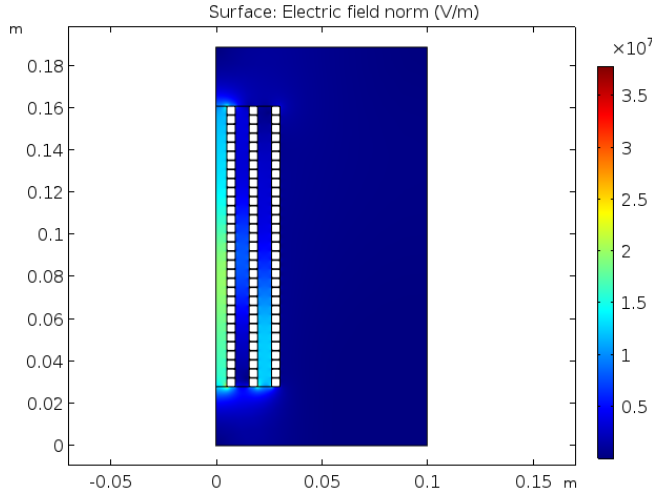


Fig. 16 Dielectric stress distribution of the transformer winding for the final geometrical configuration (Case B)

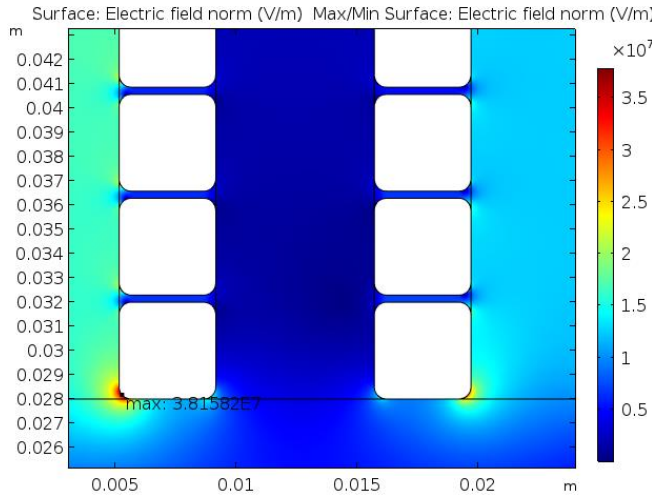


Fig. 17 Close-up to the region of maximum dielectric stress for the final geometrical configuration (Case C)

## VIII. CONCLUSIONS

This paper described a procedure to optimize the dielectric design of a power transformer winding under a fast-rising excitation. The procedure establishes an interaction between a FEM based program and a transformer winding model, to accurately calculate the parameters and transient response of the winding, with a multiobjective optimization algorithm aimed at optimizing the dielectric distances in different regions of the insulation system. The initial inputs of the problem are obtained by means of the transient voltage response produced by a fast front excitation.

The results obtained after applying the optimization procedure demonstrate the reduction of the overall dimensions of the transformer which would be reflected in a lower manufacturing cost. Most importantly, the maximum dielectric stress allowed for the insulation material is met in all cases under study, which minimizes the probability of failure once in operation.

## IX. REFERENCES

- [1] J. M. Villanueva-Ramírez, P. Gómez, F. P. Espino-Cortés and G. Nájera, "Implementation of time domain transformer winding models for fast transient analysis using Simulink," *International Journal of Electrical Power and Energy Systems*, vol. 61, no. 1, pp. 118-126, 2014.
- [2] F. P. Espino-Cortés, E. A. Cherney and S. H. Jayaram, "Impact of Inverter Drives Employing Fast-Switching Devices on Form-Wound AC Machine Stator Coil Stress Grading," *IEEE Electrical Insulation Magazine*, vol. 23, no. 1, pp. 16-28, 2007.
- [3] S. U. Haq, S. H. Jayaram and E. A. Cherney, "Evaluation of Medium Voltage Enamelled Wire Exposed to Fast Repetitive Voltage Pulses," *IEEE Transactions on Dielectrics and Electrical Insulation*, vol. 14, no. 1, pp. 194-203, 2007.
- [4] P. Gómez, F. P. Espino-Cortés and F. de León, "Computation of Dielectric Stresses Produced by PWM Type Waveforms on Medium Voltage Transformer Windings," in *IEEE Conference on Electrical Insulation and Dielectric Phenomena*, Cancún, 2011.
- [5] A. S. AlFuhaid, "Frequency Characteristics of Single-Phase Two-Winding Transformers Using Distributed-Parameter Modeling," *IEEE Transactions on Power Delivery*, vol. 16, no. 4, pp. 637-642, 2001.
- [6] Z. Luna, P. Gómez, F. P. Espino-Cortés and R. Peña-Rivero, "Modeling of Transformer Windings for Fast Transient Studies: Experimental Validation and Performance Comparison," *IEEE Transactions on Power Delivery*, vol. PP, no. 99, p. 1, 2016.
- [7] F. de León, P. Gómez, J. A. Martínez-Velasco and M. Rioual, "Chapter 4 Transformers," in *Power System Transients: Parameter Determination*, J. A. Martínez-Velasco, Ed., Boca Raton, FL: CRC Press, 2009, pp. 177-250.
- [8] P. Gomez and F. de Leon, "Impulse-Response Analysis of Toroidal Core Distribution Transformers for Dielectric Design," *IEEE Transactions on Power Delivery*, vol. 26, no. 2, pp. 1231-1238, 2011.
- [9] P. Gómez and F. de León, "Accurate an Efficient Computation of the Inductance Matrix of Transformer Windings for the Simulation of Very Fast Transients," *IEEE Transactions on Power Delivery*, vol. 26, no. 3, pp. 1423-1431, 2011.
- [10] P. Gómez and F. A. Uribe, "The numerical Laplace transform: an accurate tool for analyzing electromagnetic transients on power system devices," *Int. Journal of Electrical Power & Energy Systems*, vol. 31, no. 2-3, pp. 116-123, 2009.

TABLE V. RESULTS (CASE C)

Geometry	Distance [mm]			Maximum dielectric stress [MV/m]		
	Region I	Region II	Region III	Region I	Region II	Region III
Initial	2	5	2	62.790	41.163	62.038
Optimized	0.294	5.181	6.5644	36.512	38.158	35.829